Available online at www.sciencedirect.com
ScienceDirect
Journal of Power Sources 159 (2006) 1450–1457
JOURNAL OF POWER SOURCES
www.elsevier.com/locate/jpowsour

A new polymer electrolyte system $(PEO)_n$:$NaPO_3$

Amrtha Bhide, K. Hariharan *

Solid State Ionics Laboratory, Department of Physics, Indian Institute of Technology Madras, Chennai 600036, India

Received 21 July 2005; accepted 12 November 2005
Available online 18 January 2006

Abstract

A new Na^+ ion conducting polymer electrolyte, based on poly(ethylene oxide) (PEO) and sodium meta phosphate ($NaPO_3$) is investigated. $(PEO)_n$:$NaPO_3$ polymer metal salt complexes with different [ethylene oxide]/Na ratios ($n = 3$, 4, 6, 8 and 10) are prepared by the solution casting method. Dissolution of the salt into the polymer host is confirmed by X-ray diffraction, differential scanning calorimetry (DSC) and scanning electron microscopy. Further, interaction of the polymer chains with the metal salt is substantiated by Fourier transform infrared spectroscopy. The electrical conductivity of the samples is measured over the temperature range 322–351 K. The temperature dependent conductivity exhibits two different activation energies, below and above the softening point of the polymer. The composition $(PEO)_6$:$NaPO_3$ is found to exhibit the least crystallinity but the highest conductivity 2.8×10^{-8} S cm^{-1} at 351 K. The electronic transport number, measured by the dc polarization technique, shows that the conducting species are ionic in nature. The effect of ethylene carbonate on the best conducting composition is investigated by DSC and impedance spectroscopy. The addition of 20 wt.% ethylene carbonate, increases the amorphous phase and enhances the conductivity by two orders of magnitude.

Keywords: Polymer metal salt complex; Crystallinity; Transport number; Plasticizer; Conductivity

1. Introduction

Solvent-free, metal salt complexes belong to the class of superionic materials known as polymer electrolytes. These materials have been studied extensively in recent years, not only because of their ideal features as a solid electrolyte, but because of the transport mechanism which differs sharply from that of conventional fast-ion conductors. Polymer electrolytes have many advantages, such as flexibility, ease of processing into thin films of large surface area, electrochemical stability, leak-proof nature and volumetric stability over repeated charge–discharge cycles in a given device. These features are highly preferable for electrolytes used in numerous solid-state electrochemical devices, such as secondary batteries, electrochromic display devices, supercapacitors and specific ion sensors.

A large number of Li^+, Na^+ and H^+ conducting polymer electrolytes, formed by the dissolution of alkali metal salts in various polymer hosts have been reported in literature [1]. In order to achieve a well-complexed polymer–metal–salt system, the choice of polymer as well as the metal salt plays a key role. Nevertheless, only a few common guidelines are available for choosing the polymer host and the metal salt [2–4]. The choice of polymer host depends mainly on factors, such as: (i) the presence of a sequential polar group with large sufficient electron donor power to form coordination with cations; (ii) a low hindrance to bond rotations, there by favouring easier segmental motion; (iii) a suitable distance between coordinating centres, in order to form multiple intrapolymer ion bonds. In this context, a variety of polymers, such as poly(ethylene oxide) (PEO), poly(propylene oxide) and poly(ethylenimine), poly(ethylene succinate), have been examined as host polymers [1]. The polymer poly(ethylene oxide) has received much attention as a host polymer because of its ability to dissolve high concentrations of a wide variety of metal salts, and its good electrochemical stability and mechanical properties compared with those of other polymer hosts [1,5,6].

In order to achieve complete dissolution of salt into the polymer host, the lattice energy of the salt has to be compensated by the exothermic ion-solvation energy. This condition contributes to the reduction in the change of free energy that is involved

* Corresponding author. Tel.: +91 44 22574856; fax: +91 44 22574852.
E-mail address: khariharan@physics.iitm.ac.in (K. Hariharan).

0378-7753/$ – see front matter © 2005 Elsevier B.V. All rights reserved.
doi:10.1016/j.jpowsour.2005.11.096

in the solvation process. The choice of cation is restricted to a group of small ions, because of the requirements for the electrolyte in the given application, and hence the size of the anion plays important role in fulfilling the criterion of lattice energy. A comparison of the anions, according to the size and cation–anion tables, with respect to solubility in PEO has been well reviewed [3,7]. It is found that anions with larger radii possess least lattice energy, and those with low charge density have the least tendency to form tight ion-pairs. Therefore, the most common anions that aid complexation are I^-, SCN^-, $ClO_4{}^-$, $CF_3SO_3{}^-$, $BF_4{}^-$ and $AsF_6{}^-$. The coordination of the cations and the functional groups of the polymer and the stability of the complex depends on the Hard Soft Acid Base (HSAB) principle [1,4]. The recent developments in the filed of polymer ionics are directed towards finding a new polymer host or optimizing the ionic conductivity of well-known polymer electrolytes by several routes, such as the incorporation of nanosized inert particles and plasticizers and the blending of polymers [8].

In the present work, a new polymer electrolyte system, viz., sodium metaphosphate salt complexed with the well-known polymer host PEO, has been attempted. Though lattice energy data are not available for $NaPO_3$, the $PO_3{}^-$ ion has a radius (0.204 nm) comparable with that of $BF_4{}^-$ ion (0.205 nm), the alkali salt of which is known to form complexes with PEO [9]. $(PEO)_n$:$NaPO_3$ polymer metal salt systems ($n = 3$, 4, 6, 8, 10) have been prepared and characterized by means of X-ray diffraction (XRD), differential scanning calorimetry (DSC), followed by scanning electron microscopy (SEM) and Fourier transform infrared spectroscopy (FTIR) techniques. The conductivity of these systems and transport number measurements are also studied by ac impedance spectroscopy and dc polarization techniques. The effect of ethylene carbonate plasticizer on one of the above polymer compositions has been evaluated through DSC and ac impedance spectroscopy.

2. Experimental

Poly(ethylene oxide) (mol. wt. 4×10^6, Aldrich) was dried under vacuum at 60 °C for 8–10 h and $NaPO_3$ salt was prepared on slow cooling a melt of Na_2CO_3 and $(NH_4)H_2PO_4$ from 900 °C to room temperature. The salt was kept in an oven at 150 °C for 24 h prior to use. Polymer electrolyte films with O:Na ratios of 3, 4, 6, 8 and 10 were prepared by the solution-casting method. Appropriate quantities of PEO and $NaPO_3$ were dissolved in acetonitrile, and then thoroughly mixed and stirred for 24 h using a magnetic stirrer. The resulting homogeneous solution was poured into a PTFE Petri dish and vacuum dried at 50 °C for 48 h to remove all traces of solvent. The thin polymer films thus obtained had a thickness of about 150 μm and were preserved in a vacuum desiccator.

X-ray diffraction patterns of the $NaPO_3$ salt, PEO and polymer electrolytes in the form of films were obtained with a by Philips X-ray generator (PW140) in the range 10–60° using Cu Kα radiation. All the measurements were taken under identical conditions for unambiguous comparison. The thermal behaviour of the complexes was studied using a NETZSCZ DSC (200 Phox), over a range of −100 to 100 °C. Polymer samples of about 5–6 mg were sealed in aluminum pans and experiments were performed under a nitrogen gas atmosphere. The samples were first heated from room temperature to 100 °C (run I), cooled to −100 °C (run II), then again heated to 100 °C (run III) at a heating rate of 5 °C min^{-1}. The surface morphology of the gold coated polymer films was investigated with a JEOL scanning electron microscope (JSM 840), and FTIR absorption spectra were recorded with a Perkin-Elmer spectrometer in the frequency range of 3000–500 cm^{-1} at a resolution of 2 cm^{-1}.

Impedance measurements were taken with a Keithley 3330 impedance analyzer in the frequency range 40 Hz to 100 kHz and the data was collected through a IEEE-488 interface bus. The polymer films were cut into a circular shape of 10 mm diameter, and the silver electrodes were coated on both sides for good electrical contacts. The sample was kept between a pair of finely polished silver electrodes and the cell assembly was maintained under a constant spring load in a quartz sample holder. The temperature of the sample was maintained by a chromel–alumel thermocouple, which was kept close to the sample, with an accuracy of ±1 K. The measurements were carried out over the temperature range of 322–351 K under a nitrogen atmosphere. The electronic transference number of the polymer electrolyte was determined by means of the dc polarization method. In this method, a constant dc voltage of 200 mV was applied across the sample, which was placed between a pair of blocking silver electrodes, and the current flowing through the cell was monitored as a function of time with a Keithley 614 high impedance electrometer.

The electronic transference number was calculated using the relation:

$$t_e = \frac{I_s}{I_0} \quad (1)$$

where I_0 and I_s represent the instantaneous current on application of voltage and the resultant current at the end of polarization, respectively.

3. Results and discussion

3.1. Characterization of polymer electrolytes

A comparison of the XRD patterns of $NaPO_3$ salt and solution-cast films of pure PEO and polymer salt complexes with different O:Na ratios are presented in Fig. 1. The XRD pattern of $NaPO_3$ was compared with standard JCPDS data (11-0650) and the phase was confirmed. PEO shows two broad peaks at around 20° and 23°, which indicates the semi-crystalline nature of the polymer [6]. On addition of the salt into the polymer host, the XRD pattern of the complexes showed broadening and reduction in the intensity of the PEO peaks. This can be attributed to destruction of the ordered arrangement of the polymer side chains, and hence an enhancement in the amorphous phase. In addition, the XRD of complexes display peaks of low intensity that correspond to strong lines of $NaPO_3$. No new peaks are observed.

The DSC traces of pure PEO and a typical polymer electrolyte with a O:Na ratio of 6:1 are shown in Fig. 2. These were

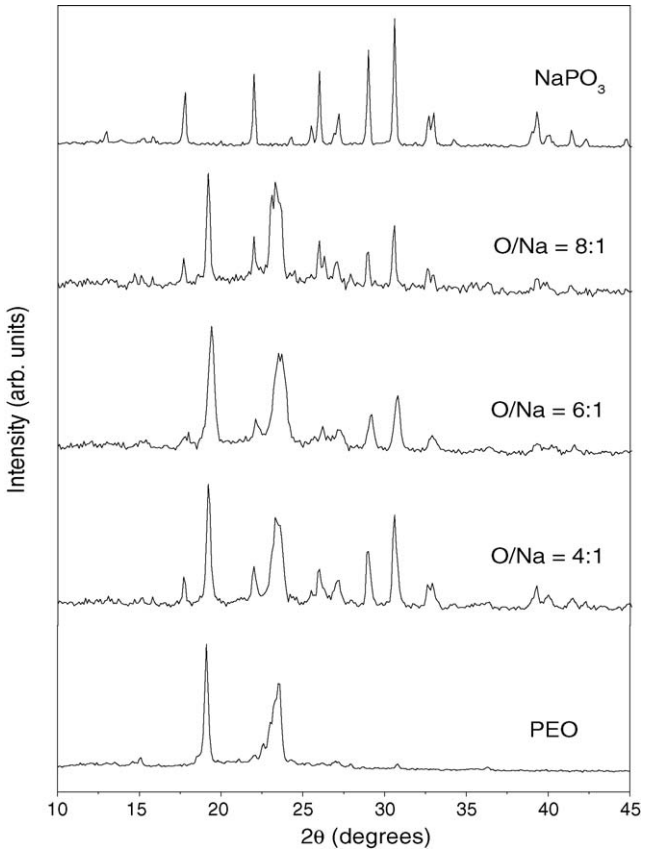

Fig. 1. X-ray diffraction patterns of PEO, $NaPO_3$ and $(PEO)_n$:$NaPO_3$ electrolytes.

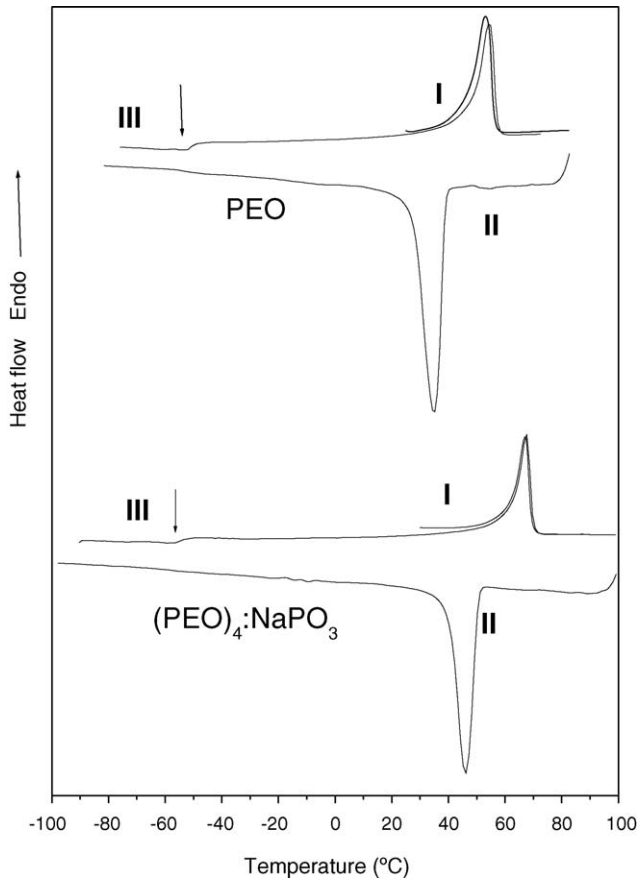

Fig. 2. DSC traces of pure PEO and $(PEO)_6$:$NaPO_3$.

recorded over a thermal cycle, in which the samples were heated from room temperature to 100 °C, cooled to −100 °C and then reheated to 100 °C. Thermal parameters, such as the glass transition temperature (T_g), the melting temperature and the degree of crystallinity obtained during the heating process from −100 to 100 °C (run III), are listed in Table 1 for pure PEO and polymer electrolyte films with different O:Na ratios. The value of T_g increases with increase in salt concentration and reaches a maximum for O:Na = 6; it then decreases. The increase in T_g can be attributed to a reduction in polymer chain flexibility due to interaction of ether oxygens in the polymer chain and Na^+ ions. This confirms complexation of the polymer and the metal salt. Similar types of variation have been observed in other systems [10]. The melting points of the polymer electrolytes are found to vary by a few degrees from that of pure PEO (63.7 °C). This reflects the presence of crystalline regions at various degrees of perfection in the complexed samples [11]. The endothermic peak above 60 °C corresponds to the melting point of the pure PEO crystalline phase. The polymer–salt interaction caused by the addition of salt causes disorder in the oriented crystalline-rich phase. The crystallinity of a complex is calculated from:

$$X_C = \frac{\Delta H_m}{\Delta H^0_{PEO}} \quad (2)$$

where ΔH_m is the enthalpy of melting of the sample and ΔH^0_{PEO} is the enthalpy of melting of 100% crystalline PEO, namely 213.7 J g^{-1} [12]. The crystallinity of the composition with the lowest salt concentration (O:Na ratio 10) is found to be least affected. On increasing the salt content, however the crystallinity reduces to a minimum of 37% for a O:Na ratio of 6, compared with 63% for the polymer host. On further increase in the salt concentration, the crystallinity increases and this can be attributed to either a crystalline-rich phase or a uncomplexed salt-rich phase.

Table 1
Comparison of thermal parameters of $(PEO)_n$:$NaPO_3$ systems

Composition O:Na ratio	T_g (°C)	T_m (°C)	Crystallinity (%)
Pure PEO	−61.1	63.7	63.1
10	−58.8	67.2	54.7
8	−55.4	66.8	44.5
6	−53.1	62.3	37.4
4	−54.1	67.1	40.5

Scanning election micrographs of uncomplexed PEO and polymer metal salt complexes with O:Na ratios of 4, 6, 8 and 10 are presented in Fig. 3a–e. The micrograph of pure PEO shows only bright and dark regions in the form of stripes, which correspond to the crystalline and amorphous phases of the polymer film. On addition of the salt, the dark area corresponding to the amorphous phase increases, which indicates a reduction in crystallinity of the polymer electrolytes. The polymer electrolyte with a O:Na ratio of 10, i.e. the least salt concentration,

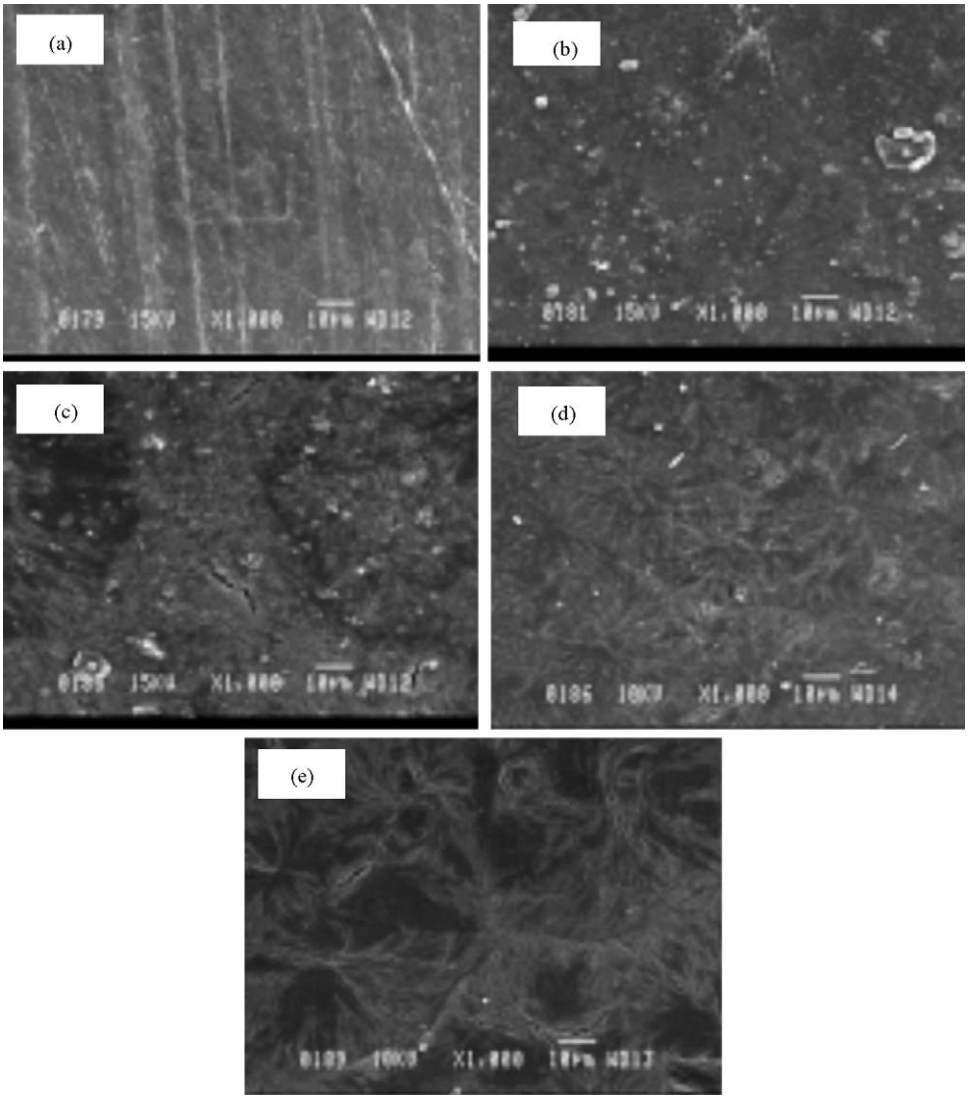

Fig. 3. Scanning electron micrographs: (a) pure PEO, (b) O:Na = 4, (c) O:Na = 6, (d) O:Na = 8, (e) O:Na = 10.

has a distinct, uniformly arranged, spherulite-like structure. On increasing the salt concentration, the weak fibrillar branches found in the spherulitic structure are markedly diminished and appear to be spherulitic nuclei. At the maximum salt concentration, i.e. O:Na = 4, micrograph shows a zone of uncomplexed salt, together with crystalline and amorphous regions of the polymer. These morphological studies substantiate the results obtained by XRD and DSC techniques with regard to complexation and enhancement of the amorphous phase of the polymer.

On addition of salt to the polymer host, the cation of the metal salt becomes coordinated with ether oxygen of the polymer backbone and give rise to in complexation. This type of interaction will influence the local structure of the polymer backbone and certain infrared-active modes of vibration will become affected. In this context, various groups have confirmed the complexation of alkali metal salts in polymer hosts, by the FTIR technique [13–16]. The FTIR spectra of $NaPO_3$ and thin films of PEO and $(PEO)_n$:$NaPO_3$ polymer metal complexes with different O:Na ratios are shown in Fig. 4. The spectra of the complexed systems display some spectral features that are similar to those of pure PEO. Prominent changes have been observed in the following spectral regions, due to the polymer–metal salt interaction.

(i) In the spectral range 1050–1160 cm^{-1}, significant changes are observed in the width and the intensity of the vibrational bands of PEO, on the addition of $NaPO_3$ at different concentrations. These conformal changes correspond to C–O–C symmetric vibrational modes. In addition, a few low intense bands are observed in the range 800–1000 cm^{-1}. The conformal changes, which correspond to those of IR active vibrational bands involving ether oxygen, indicate the complexation of alkali metal ion to the ether oxygen [13,14].

(ii) The width of the strong absorption band of the C–H stretching modes seen in the region 2800–2950 cm^{-1} decreases with increasing salt concentration.

(iii) The rest of the bands in the above range are found to be similar to those of PEO. This confirms that the guche CO–CO conformation of pure PEO remains unaffected on complexation. Similarly, the vibrational bands seen in the range

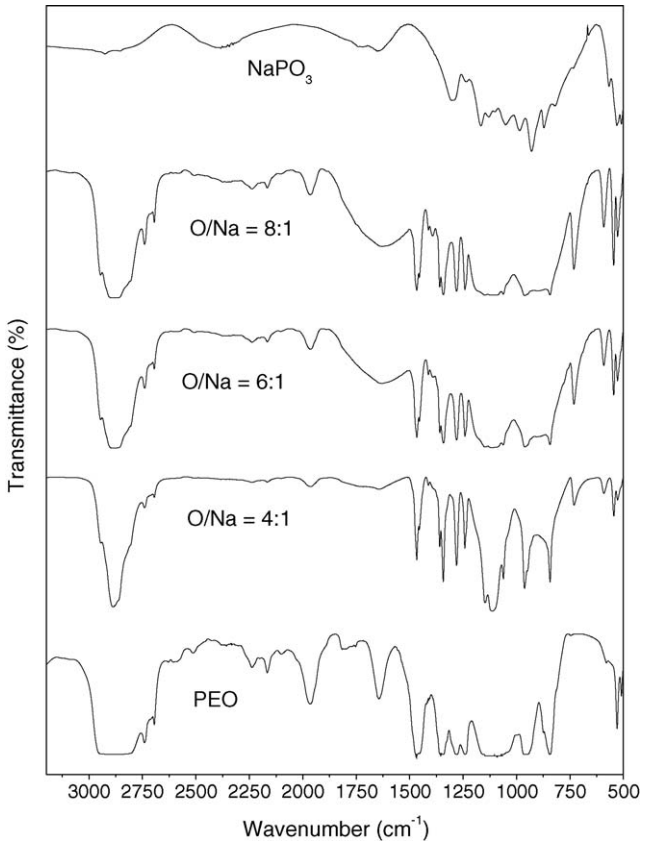

Fig. 4. FTIR spectra of PEO, $NaPO_3$ and $(PEO)_n$:$NaPO_3$ polymer electrolytes.

1242–1280 cm^{-1}, which are assigned to CH_2 wagging modes, and those observed between 992 and 1012 cm^{-1}, which are assigned to CH_2 rocking remain unchanged [13]. Though a detailed analysis has not been carried out because of the poor resolution of the spectra, the above observations confirm the complexation.

3.2. Conductivity studies

Conductivity measurements of the above polymer electrolyte samples have been carried out as a function of temperature. The samples were heated to 351 K and measurements were carried out while cooling the sample. Impedance plots of the $(PEO)_6$:$NaPO_3$ polymer electrolyte system as a function of temperature are given in Fig. 5. The plots show a depressed semicircular nature and an increase in radius with decrease in temperature, which indicates an activated conduction mechanism. The plots have been analyzed by means of the EQUIVCRT non-linear least-squares fitting program [17] and the bulk resistance has been extracted in order to determine the conductivity. The same procedure was adopted for determination of the conductivity of different compositions. The inset of Fig. 5 shows the conductivity as a function of frequency at various temperatures. In the low-frequency range, the conductivity is independent of frequency. By contrast conductivity dispersion is observed at higher frequency ranges. As the temperature increases, the frequency at which the dispersion becomes prominent shifts to a higher frequency region.

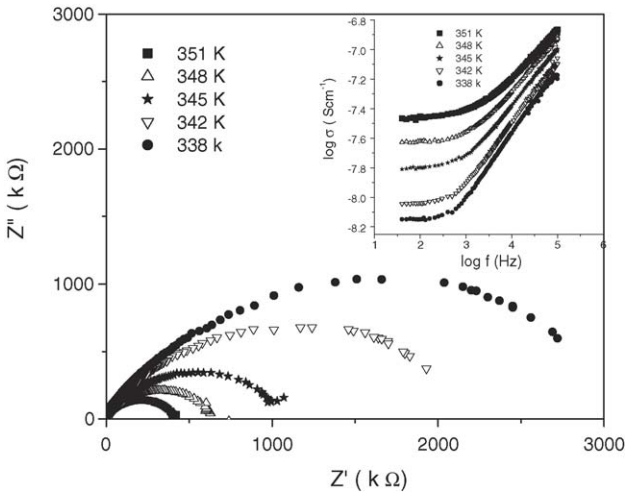

Fig. 5. Impedance plots of $(PEO)_6$:$NaPO_3$ polymer electrolyte system. *Inset*: Frequency-dependent conductivity plot.

Though the conductivity of the polycrystalline $NaPO_3$ salt is not available, the conductivity of the palletized salt is found to be less than 10^{-9} S cm^{-1} under an inert atmosphere at room temperature. On the other hand, the $(PEO)_6$:$NaPO_3$ system exhibits a maximum conductivity of 2.8×10^{-8} S cm^{-1} at 351 K, which is above the softening point of the polymer electrolyte system. On further increasing or decreasing the salt concentration, the conductivity decreases. In the case of polymer electrolyte systems, the elastomeric phase favours the migration of carrier ions via micro-Brownian motion of the polymer segments. Also, the ions find easier pathways in interchain and intrachain polymer segments, which favours an enhancement in conductivity [18,19]. The temperature dependent conductivity of polymer electrolytes with different O:Na ratios is shown in Fig. 6. The graphs obey Arrhenius behavior with a clear distinction in the slopes around 338 K, above which the polymer metal salt complex starts to soften. This feature indicates that the polymer–metal complex has a crystalline phase throughout the temperature range. Similar features have been observed for a PEO-NaSCN system by Armand et al. [20]. The plots are fitted to the relation

$$\sigma = \sigma_0 \exp\left(\frac{-E_a}{K_B T}\right) \quad (3)$$

using linear fit program, where σ_0 is the pre-exponential factor, E_a the activation energy, K_B the Boltzmann constant and T is the absolute temperature. The activation energy and conductivity values in the two regions are given in Table 2. All the samples consistently show higher conductivity above the softening point with a low activation energy, which demonstrates that the amorphous phase is responsible for ionic conduction.

3.3. Transport number measurement

The sample was placed between a pair of silver blocking electrodes and maintained at 351 K for 2 h. On application of a dc potential of 200 mV to the above configuration, the instantaneous initial current I_0, is 0.13 μA. After a long interval of 18 h,

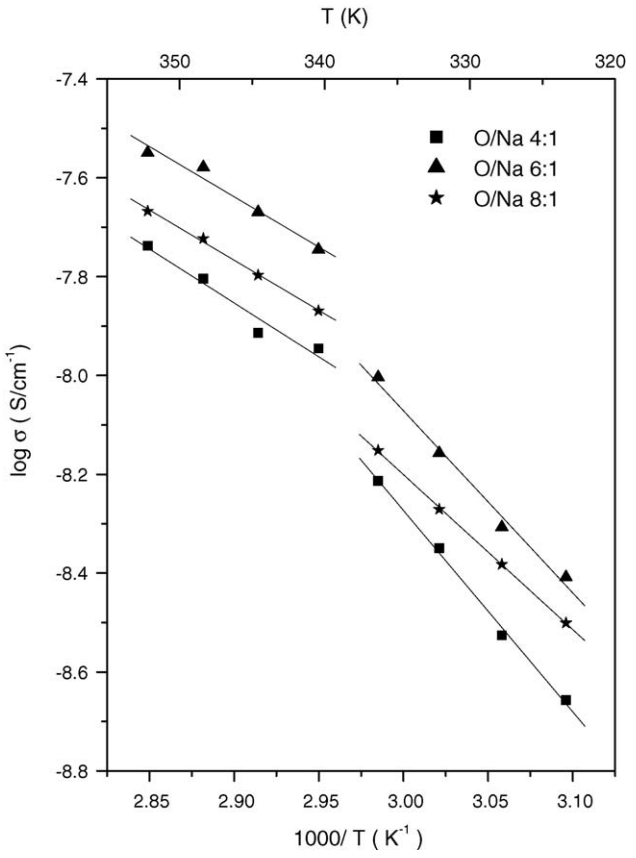

Fig. 6. Temperature-dependent conductivity of different composition.

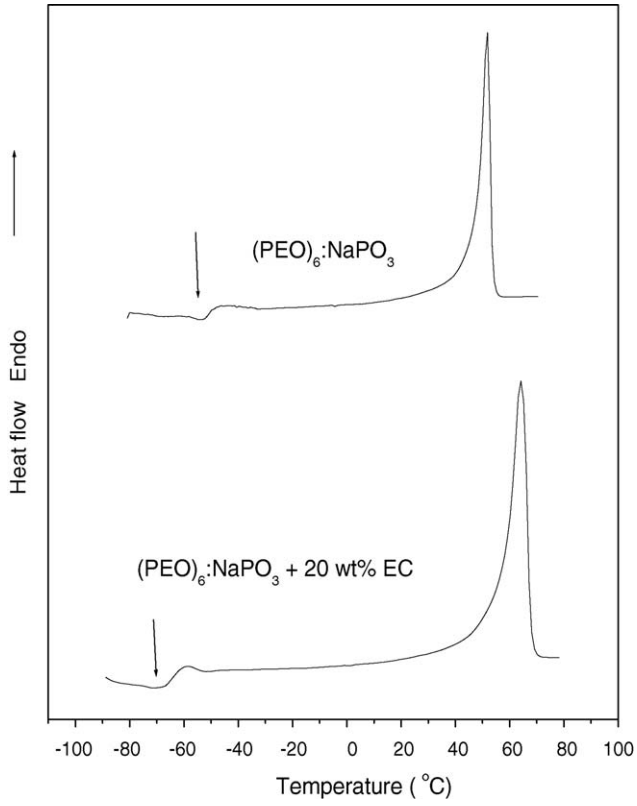

Fig. 7. DSC traces of $(PEO)_6$:$NaPO_3$ polymer electrolyte and plasticized electrolyte.

the cell because completely polarized and delivered a steady-state current of 1.8 nA.

There was no significant change in the above value even after 48 h. The decrease in the polarization current can be attributed to the migration of ions due to the applied field and this is balanced by diffusion due to the concentration gradient. Thus, the resulting steady-state current is due only to electrons or holes and the electronic contribution is found to be 0.01. The ionic contribution is evaluated through the equation [21]:

$$t_i = 1 - \frac{I_s}{I_0} \quad (4)$$

and is found to be nearly equal to unity.

4. Effect of plasticizer on $(PEO)_6$:$NaPO_3$

The effect of plasticizer addition on the conduction characteristics of the best conducting $(PEO)_6$:$NaPO_3$ polymer electrolyte system has been investigated. Ethylene carbonate was chosen because of its high dielectric constant and viscosity, which favours ionic dissociation of the solute and easy ion migration [22]. 20 wt.% of ethylene carbonate (Aldrich, 98%) was incorporated while homogenizing a acetonitrile solution of PEO and $NaPO_3$ at a O:Na ratio of 6. Thin films of the polymer electrolytes were obtained by the solution-casting method, as explained above.

The DSC traces of $(PEO)_6$:$NaPO_3$ + 20 wt.% EC and $(PEO)_6$:$NaPO_3$ polymer electrolytes are given in Fig. 7. The results reveal a decrease in the degree of crystallinity to 34.1% and a lowering of the T_g to −66.7 °C, which can be attributed to an enhancement in the amorphous phase and improved flexibility of the polymer host.

A comparison of temperature-dependent conductivities of $(PEO)_6$:$NaPO_3$ and plasticized polymer electrolyte is shown in Fig. 8. The plasticized electrolyte has a conductivity of 1.6×10^{-6} S cm^{-1} at 351 K, which is two orders of magnitude

Table 2
Temperature-dependent conductivity and activation energy as function of composition

Composition O:Na ratio	Conductivity at 322 K (S cm^{-1})	E_a (eV) region below 338 K	Conductivity at 351 K (S cm^{-1})	E_a (eV) region above 338 K
10	1.2×10^{-9}	0.71	1.6×10^{-8}	0.43
8	3.2×10^{-9}	0.69	2.2×10^{-8}	0.40
6	3.9×10^{-9}	0.73	2.9×10^{-8}	0.40
4	1.4×10^{-9}	0.81	1.9×10^{-8}	0.43
3	1.9×10^{-9}	0.74	0.6×10^{-8}	0.44

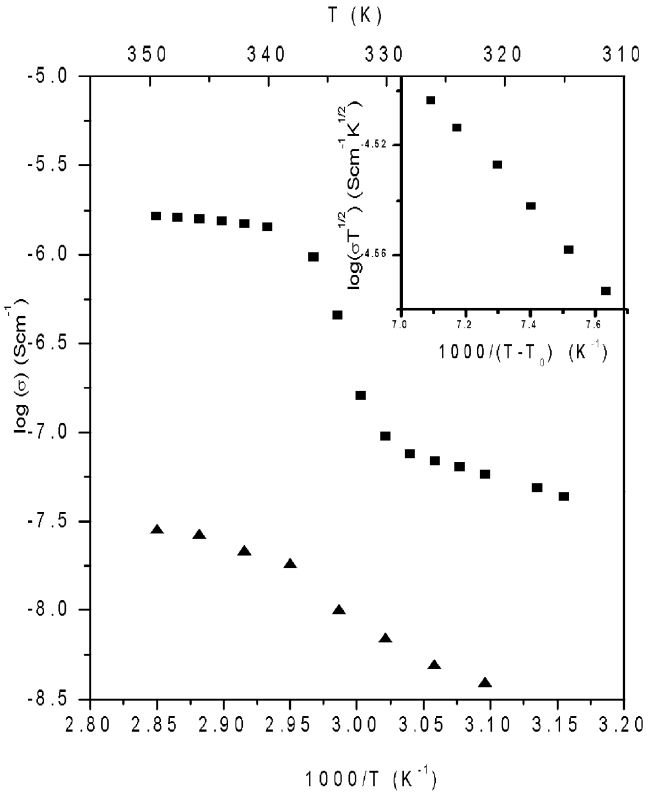

Fig. 8. Comparison of temperature-dependence of conductivity of $(PEO)_6$:$NaPO_3$ and plasticized $(PEO)_6$:$NaPO_3$ with 20 wt.% of ethylene carbonate. *Inset*: VTF plot of plasticized polymer electrolyte above softening point.

higher than that of the $(PEO)_6$:$NaPO_3$ system. In contrast to the PEO–$NaPO_3$ system, the temperature-dependent conductivity plot has exhibits curvature above the softening point. This type of behaviour is often displayed by polymer metal salt complexes with elastomeric-rich phase and is conventionally described by the empirical Vogel–Tammann–Fulcher (VTF) equation [23–26], i.e.

$$\sigma(T) = AT^{-1/2} \exp\left\{-\frac{B}{T - T_0}\right\} \quad (5)$$

where T is the absolute temperature, and A, B and T_0 are the fitting constants. The fitting constant A includes some terms that might show temperature dependence, B is considered as the pseudoactivation energy. T_0 is the Vogel temperature or ideal glass transition temperature, at which the free volume of the polymer tends to zero.

The data has been fitted to the Eq. (5), following the fitting procedure explained by Adamic et al. [27]. The inset of Fig. 8 shows a linear plot obtained by plotting log $(\sigma T^{1/2})$ versus $1000/(T - T_0)$, for the conductivity data above the softening temperature. The pseudo activation energy determined from the best fitting parameters at $T_0 \cong T_g$ (205 K) is found to be 0.03 eV. It is noted that the conductivity data below the softening temperature exhibits an Arrhenius type behaviour, with an activation energy of 0.41 eV.

5. Conclusions

PEO-based polymer electrolytes complexed with $NaPO_3$ have been prepared by the solution-casting method. Polymer metal salt complexes with different O:Na ratios have been characterized by XRD, DSC and SEM studies. The broadening and reduction in the intensity of the Bragg peaks confirms the dissolution of metal salt in the polymer host. The DSC results have further confirmed a reduction in the crystallinity and an increase in the T_g of polymer electrolytes, compared with that of pure PEO. Also, scanning electron micrographs distinctly show the morphology of both uncomplexed polymer and polymer complexed with $NaPO_3$. Conformal changes in the infrared-active modes of the polymer side chains indicate the coordination of the ether oxygen of PEO with the metal salt ion. The electrical conductivity of the above electrolytes proceeds via an activated conduction mechanism with two different activation energies. The $(PEO)_6$:$NaPO_3$ system with an elastomeric-rich phase exhibits a maximum conductivity of 2.8×10^{-8} S cm^{-1}, with a negligible electronic transport number. Therefore, this material establishes a new polymer electrolyte system, $(PEO)_n$:$NaPO_3$. Incorporation of 20 wt.% of ethylene carbonate as the plasticizer increases the amorphous phase and enhances the conductivity by two orders. Thus, the plasticized $(PEO)_6$:$NaPO_3$ polymer electrolyte system with an enhanced amorphous phase and conductivity requires further investigation for device applications.

References

[1] P.G. Bruce, Solid State Electrochemistry, Cambridge University Press, Cambridge, 1995.
[2] J.R. MacCallum, C.A. Vincent, Polym. Electrolyte Rev., vol. 1, Elsevier, 1989.
[3] C.A. Vincent, Prog. Solid State Chem. 17 (1987) 145–261.
[4] F.M. Gray, Polymer Electrolytes: Fundamentals and Technological Applications, VCH publications, New York, 1991.
[5] D. Baril, C. Michot, M. Armand, Solid State Ionics 97 (1997) 35–47.
[6] P.G. Bruce, C.A. Vincent, J. Chem. Soc. Faraday Trans. 89 (1993) 3187–3203.
[7] M.A. Ratner, D.F. Shriver, Chem. Rev. 88 (1988) 109–124.
[8] M.M.E. Jacob, E. Hackett, E.P. Giannelis, J. Mater. Chem. 13 (2003) 1–5.
[9] R. Dupon, B.L. Papke, M.A. Ratner, D.H. Whitmore, D.F. Shriver, J. Am. Chem. Soc. 104 (1982) 6247–6251.
[10] C.A. Angell, C. Liu, E. Sanchez, Nature 362 (1993) 137–139.
[11] M.D. Glasse, R.J. Latham, R.G. Linford, W.S. Schlindwein, A. Careem, Solid State Ionics 72 (1994) 127–134.
[12] J.H. Shin, K.W. Kim, H.J. Ahn, J.H. Ahn, Mater. Sci. Eng. B 95 (2002) 148–156.
[13] B.L. Papke, M.A. Ratner, D.F. Shriver, J. Electrochem. Soc. 129 (1982) 1434–1438.
[14] S.J. Wen, T.J. Richrdson, D.I. Ghantous, K.A. Striebel, P.N. Ross, E.J. Cairns, J. Electroanal. Chem. 408 (1996) 113–118.
[15] M.A.K.L. Dissanayake, R. Frech, Macromolecules 28 (1995) 5312–5319.
[16] P.S. Anantha, K. Hariharan, Solid State Ionics 176 (2005) 155–162.
[17] B.A. Boukamp, Equivalent Circuit, University of Twente, The Netherlands, Report No. CT128/88/CT112/89, 1989.
[18] M. Watanabe, N. Ogata, Brit. Poly. J. 20 (1988) 181–192.
[19] C.A. Vincent, Chem. Brit. 25 (1989) 391–395.
[20] M.B. Armand, J.M. Chabango, M.J. Duclot, in: P. Vashishta, J.N. Munday, G.K. Shenoy (Eds.), Fast Ion Transport in Solids, North-Holland, Arsterdam, 1979, pp. 131–136.
[21] N. Srivastava, A. Chandra, S. Chndra, Phys. Rev., B 52 (1995) 225–230.

[22] S.-I. Tobishima, A. Yamaji, Electrochim. Acta 29 (1984) 267–271.
[23] H. Vogel, Phys. Z. 22 (1921) 645.
[24] G. Tamman, E.W. Hesse, Z. Anorg, Allg. Chem. 156 (1926) 245.
[25] G.S. Fulcher, J. Am. Ceram. Soc. 8 (1925) 339.
[26] M.H. Cohen, D. Turnball, J. Chem. Phys. 31 (1959) 1164–1169.
[27] K.J. Adamic, S.G. Greenbaum, M.C. Wintersgill, J.J. Fontanella, J. App. Phys. 60 (1986) 1342–1345.